




Digital Models for Power Flow Analysis and Calculation of Electromagnetic Interference Effects of Long-Distance Ultrahigh-Voltage Transmission Lines

Andrey Kryukov^{1,2}^a, Konstantin Suslov^{1,3}^b and Alexandr Kryukov¹^c

¹Department of Power Supply and Electrical Engineering, Irkutsk National Research Technical University, Irkutsk, Russia

²Department of Transport Electric Power, Irkutsk State Transport University, Irkutsk, Russia

³Department of Hydropower and Renewable Energy, National Research University, "Moscow Power Engineering Institute", Moscow, Russia

Keywords: Long-Distance Ultrahigh-Voltage Transmission Lines, Comprehensive Modeling in the Phase Frame of Reference.


Abstract: The goal of the research presented in this article was to develop computer models of long-distance ultra-high voltage (UHV) power transmission lines to provide comprehensive modeling of power flows and calculating electromagnetic interference effects on extended steel structures. In developing the models, we employed the methods based on the use of the phase frame of reference and equivalent lattice circuits with a fully connected topology. The simulations were carried out for a 1,150 kV UHV transmission line with a length of 900 km, each phase of which was formed by eight AC-330 wires. Simulations were performed using the software package Fazonord. Along with power flow calculations and determination of the voltages created by the 1,150 kV long-distance transmission line on the pipeline, we simulated electromagnetic fields, taking into account the impact exerted by the grounded steel structure. The results of modeling a long-distance 1,150 kV transmission line with receiving end loads of $300 + j 200$ MVA per phase led to the following conclusions: in the case of a normal power flow with balanced loads at individual points of the structure the levels of induced voltages did not exceed the allowable limit of 60 V; in the case of two-phase and single-phase short-circuit power flows the maximum induced voltages also did not exceed the 1,000 V limit set by the regulatory document. The models presented in the paper can be put into practice when planning the measures to ensure the electrical safety of technicians working at the pipeline sections located in the areas that are subject to electromagnetic interference effects of transmission lines. The application scope of the technique developed covers the cases where a transmission line and a pipeline run in close proximity following a complex trajectory that includes parallel and oblique segments.


1 INTRODUCTION


The current stage of electric power industry development is characterized by commissioning of long-distance ultrahigh-voltage (UHV) DC and AC transmission lines. An example of such a power transmission line is the 1,000 kV line, which serves as a power bridge between the northern and central regions of the PRC (Li, 2013). The long-distance UHV transmission line projects that serves as the backbone of the Northeast Asia power

interconnection are under discussion (Podkovaalnikov, 2015). Against the current background of large-scale use of information technology, the operation of such power transmission lines calls for digital models that provide a proper power flow analysis of electric power systems (EPS) (Bulatov, 2022), in which such UHV power transmission lines are employed.

The relevance of the task of modeling of long-distance UHV transmission lines is attested by a large body of published research on the subject. For example, article (Wang, 2021) presented the results

^a <https://orcid.org/0000-0001-6543-1790>

^b <https://orcid.org/0000-0003-0484-2857>

^c <https://orcid.org/0000-0003-3272-5738>

of the study of utility frequency overvoltages and measures for its suppression in ultra-high voltage transmission lines. Study (Shao, 2012) dealt with the analysis of overvoltages arising during single-phase automatic reclosing in long-distance UHV transmission lines. The issues of overvoltage limitation in long-distance 1,000 kV transmission line were considered in article (Wang, 2018). The problem of matching the insulation of a half-wavelength ultra-high voltage transmission line was solved in (Zhang, 2020). In study (Golov, 2020) its authors described an adjustable sequential compensation installation proposed by them, which provided an increase in the transmission capacity of long-distance transmission lines. Works (Xue, 2011 a, Xue, 2011 b) were devoted to the study of switching overvoltages in long-distance UHV transmission lines. Based on the results obtained, the authors proposed measures to reduce them. The system of transmitting energy over long distances from a solar power plant was discussed in article (Rahul, 2020). Distance protection with a traveling wave for an UHV line, implemented on the basis of the wavelet transform, was proposed in (Long, 2018). Article (Dias, 2011) dealt with the issues of transmitting bulk power over extra-long distances. Flexible systems for transmitting electricity over long distances were proposed in (Davydov, 2019). Theoretical aspects of long-distance power transmission were discussed in research monographs (Aleksandrov, 2006, Ryzhov, 2007).

Our analysis of published research reveals that the tasks of complex modeling of power flows and determining the electromagnetic fields (EMF) of long-distance UHV lines and their effects on adjacent conductive facilities have not been solved to the extent warranted by the problem. This is due to the fact that in most cases the single-line approach is used to model long-distance transmission lines (Aleksandrov, 2006, Ryzhov, 2007, Zakaryukin, 2005), which makes it difficult to take into account longitudinal and transverse imbalances in power systems.

The methods for calculating power system power flows and computer technologies proposed in (Zakaryukin, 2005, Zakaryukin, 2020) allow implementing a proper and comprehensive approach to the modeling of electric networks with long-distance transmission lines and ultra-high voltage. Below we present the results of research aimed at furthering the development of techniques for modeling power flows, EMF of long-distance transmission lines and their electromagnetic interference effects (EMIE) on extended steel structures.

2 METHODOLOGY

The study of power flows, EMF and EMIE was carried out by simulating a transmission line with a nominal voltage of 1,150 kV and a length of 900 km. For simulation purposes we used the parameters of the line "Itat - Barnaul - Ekibastuz - Kokshetau - Kustanai - Chelyabinsk", built in 1980 - 1988, which now operates at 500 kV. The design transmission capacity of this line was 5,500 MW. The line used split phases made with eight AC-330 wires.

The Fazonord software package (Zakaryukin, 2020) was used as the main tool for carrying out computer-aided power flow analysis of the long-distance UHV transmission line. In order to capture the changes in currents and voltages along the length of the transmission line, the line model was partitioned into eleven elements. The first five of them corresponded to sections that were each 10 km long. The models of these sections included a segment corresponding to the above-ground pipeline, running parallel to the line at a distance of 50 m from the axis of the transmission line. The diameter of the pipe was assumed to be 250 mm. Stationary earth electrodes with a 1 Ohm leakage resistance were installed along the edges of the structure. In addition, the distributed grounding of the pipe with a conductivity of 0.05 S/km was taken into account. The length of the sixth section was 100 km, and that of the rest - 150 km. Provision was made for the transposition of line phases.

To take into account the distributive nature of parameters of the transmission line and the grounded pipeline, ladder equivalence circuits of sections consisting of series-connected multipoint devices were formed (Zakaryukin, 2005, Zakaryukin, 2020, Kryukov, 2022).

The algorithm for forming a ladder diagram included the following steps:

1) the maximum length of the short section was taken equal to a quarter of the thickness of the skin layer in the ground

$$\Delta = \sqrt{\frac{1}{\pi f \gamma \mu_r \mu_0}}, \quad (1)$$

where γ – ground conductivity, S/m; $\mu_r = 1$; f – frequency; $\mu_0 = 4\pi \cdot 10^{-7}$ Гн/м ;

2) the value of the length l was determined so as to satisfy the condition $l2^n = L$, where n - the number of sections connected in series; L – the length of the simulated line;

3) an equivalent lattice circuit (ELC) was generated for the section with length l ;

4) a ladder circuit was formed of $2n$ ELCs of sequentially connected sections; the node numbers at the beginning of the i -th section were taken equal to the numbers at the end of the $i-1$ section;

5) intermediate nodes of the generated circuit were removed and renumbered;

6) steps 4 and 5 of the algorithm were repeated n times.

The removal of the intermediate node was performed on the basis of the transformation of a star polygon into a polygon. It should be noted that the described procedure led to an increase in the number of branches of the resulting ELC.

This procedure can be illustrated using the diagram shown in Fig. 1. In the diagram, we removed the node numbered 0, to which the ground shunt with the conductivity $\underline{Y} = \frac{1}{\underline{Z}_0}$ and N branches with impedances $\underline{Z}_1, \underline{Z}_2, \dots, \underline{Z}_N$ were connected.

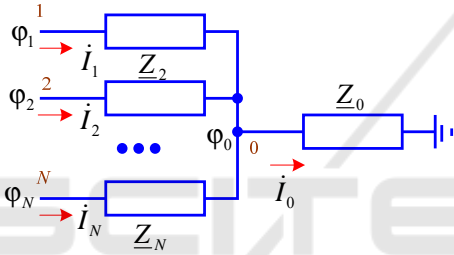


Figure 1: Transformed section of the circuit.

Branch currents can be found on the basis of their potentials:

$$i_1 = \frac{\phi_1 - \phi_0}{\underline{Z}_1}; i_2 = \frac{\phi_2 - \phi_0}{\underline{Z}_2}; \dots; i_N = \frac{\phi_N - \phi_0}{\underline{Z}_N} \quad (2)$$

Then the following relationship can be written for the potential of the node to be removed:

$$\phi_0 = \frac{i_0}{\underline{Y}} = \frac{\sum_{i=1}^N i_i}{\underline{Y}} = \frac{1}{\underline{Y}} \left(\sum_{i=1}^N \frac{\phi_i}{\underline{Z}_i} - \phi_0 \sum_{i=1}^N \frac{1}{\underline{Z}_i} \right), \quad (3)$$

from which it follows that

$$\phi_0 = \frac{1}{\underline{Y} + \sum_{i=1}^N \frac{1}{\underline{Z}_i}} \sum_{i=1}^N \frac{\phi_i}{\underline{Z}_i}. \quad (4)$$

By introducing the notation

$$\underline{Y}_0 = \underline{Y} + \sum_{i=1}^N \frac{1}{\underline{Z}_i}, \quad (5)$$

for the $k-0$ branch current, the following expression can be obtained:

$$i_k = \frac{1}{\underline{Z}_k} \left(\phi_k - \frac{\phi_1}{\underline{Y}_0 \underline{Z}_1} - \frac{\phi_2}{\underline{Y}_0 \underline{Z}_2} - \dots - \frac{\phi_k}{\underline{Y}_0 \underline{Z}_k} - \dots - \frac{\phi_N}{\underline{Y}_0 \underline{Z}_N} \right) \quad (6)$$

It follows from the above that at each of the nodes in question a shunt appeared with a conductivity of

$$\underline{Y}_k = \frac{1}{\underline{Z}_k} \left(1 - \frac{1}{\underline{Y}_0} \sum_{i=1}^N \frac{1}{\underline{Z}_i} \right). \quad (7)$$

Furthermore, additional branches were formed between the nodes, the resistances of which are defined as follows:

$$\begin{aligned} -\frac{\phi_j}{\underline{Z}_k \underline{Y}_0 \underline{Z}_j} &= -\frac{\phi_j}{\underline{Z}_k \underline{Y}_0 \underline{Z}_j} + \frac{\phi_k}{\underline{Z}_k \underline{Y}_0 \underline{Z}_j} - \frac{\phi_k}{\underline{Z}_k \underline{Y}_0 \underline{Z}_j} = \\ &= -\phi_k \frac{1}{\underline{Z}_k \underline{Y}_0 \underline{Z}_j} + \frac{\phi_k - \phi_j}{\underline{Z}_k \underline{Y}_0 \underline{Z}_j} \end{aligned} \quad (8)$$

From the above it follows that for the resistance of the branch $k-j$ we can write

$$\underline{Z}_{kj} = \underline{Z}_k \underline{Y}_0 \underline{Z}_j \quad (9)$$

In the transformed circuit there was no node 0. However, a shunt to ground appeared in each of the nodes connected to it. The circuit was complemented by $N(N-1)/2$ branches, corresponding to the connections of node 0 to adjacent nodes.

The resulting ladder diagram makes it possible to properly simulate any long-distance transmission line, as well as grounded current-carrying parts, correctly accounting for the distributed nature of parameters

3 RESULTS OF MODELING

The network schematic is shown in Fig. 2, the spatial arrangement of wires is shown in Fig. 3, the display of transformer and transmission line models in the main window of the software package is shown in Fig. 4 and 5, the simulation results - in Figs. 6 to 22.

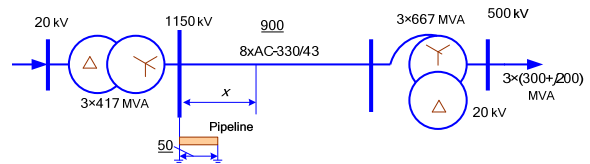


Figure 2: Network schematic: x - distance from the sending end of the transmission line.

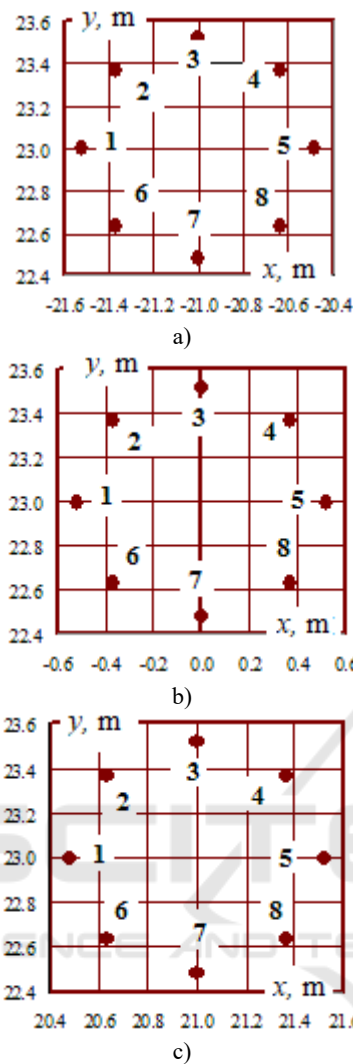


Figure 3: Coordinates of wires location: a - left phase; b - middle phase; c - right phase; bold numbers indicate wire numbers.

At the receiving end of the transmission line, a balanced load of $300 + j200$ MVA per phase was assumed. The distribution of currents over the wires at the beginning of the head section of the transmission line is shown in Fig. 6. In order to ensure that the voltage deviations are contained within the permissible limits, it was necessary to install shunt reactors, the parameters of which are shown in Fig. 7b. A model of the controlled reactive power source was installed at the receiving end of the long-distance transmission line, which provided stabilization of phase voltages at 664 kV.

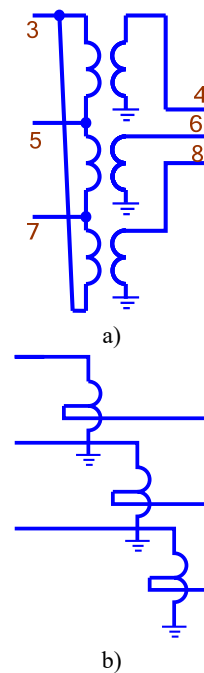


Figure 4: Models of transformers and autotransformers: a - 3x417 MVA transformer, b - 3x667 MVA autotransformer.

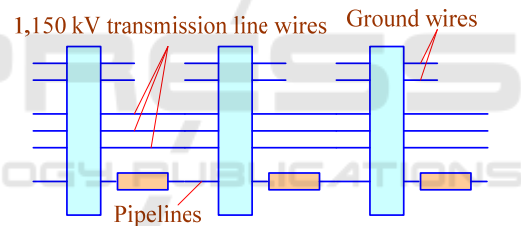


Figure 5: Detail of the visual representation of the computational model, including the UHV transmission line and the above-ground pipeline.

Power losses by sections of the transmission line are shown in Fig. 7a; the losses at sections 1...6 were summed up to obtain the same length. Fig. 7a shows that the relationship $\Delta P = \Delta P(x)$ has a minimum, corresponding to the eighth segment with coordinates $x = 300$ km at the beginning and $x = 450$ km at the end. Specific power losses per kilometer of the transmission line were in the range of 8.6 to 16.4 kW. The losses as a percentage of the transmitted active power were in the range 0.14...0.27%.

Fig. 8 shows the dependencies of asymmetry coefficients along the reverse (k_{2v}) and zero (k_{0v}) sequences on the x -coordinate, from which we can see that there is insignificant asymmetry at long-distance transmission line nodal points, which does not exceed the permissible limits.

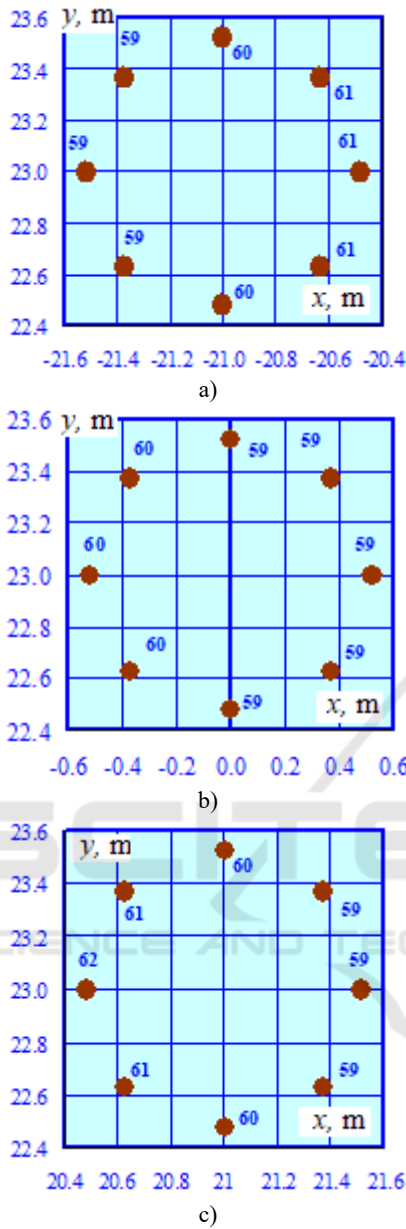


Figure 6: Distribution of currents along the wires at the beginning of the head section of the transmission line: the bold numbers indicate the numbers of wires according to Fig. 2.

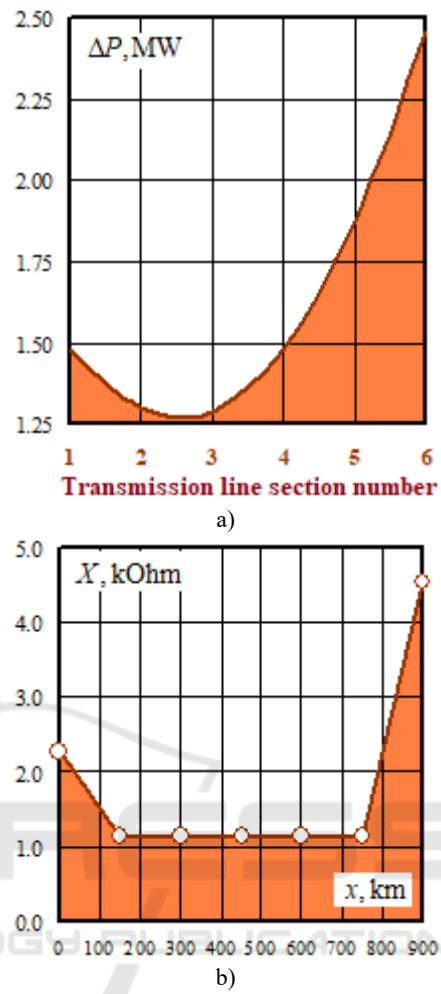


Figure 7: Power losses along sections of the transmission line (a) and inductance of shunt reactors (b) reduced to $1,150/\sqrt{3}$ kV.

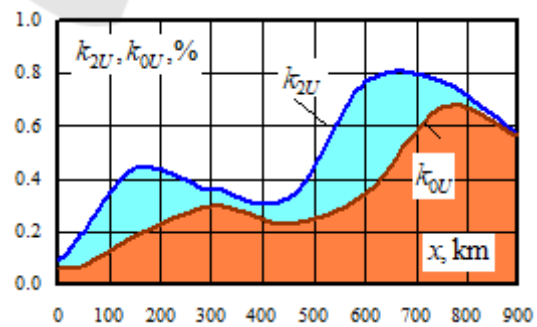


Figure 8: Asymmetry coefficients on the inverse (k_{2U}) and zero (k_0) sequences as a function of the x -coordinate.

Fig. 9 shows plots of voltage dependencies of the 1,150 kV transmission line on the x -coordinate plotted for sections 1-5 that were adjacent to the pipeline. The above plots show the decrease of

voltages with the increasing the x -coordinate; at the same time, the intensity of their decrease, which can be estimated by the ratio of increments $\frac{\Delta U}{\Delta x}$, increases. It should be noted that dependencies $\frac{\Delta U}{\Delta x} = f(x)$ are linear in nature. The plots $I = I(x)$ presented in Fig. 10 show an increase in currents as the x -coordinate increases. The parameter corresponding to the intensity of their increase grows linearly.

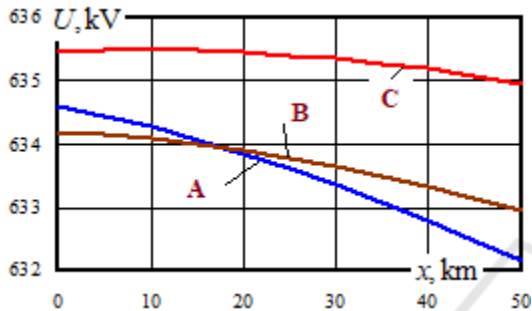


Figure 9: Voltages of the 1,150 kV transmission line as a function of the x -coordinate.

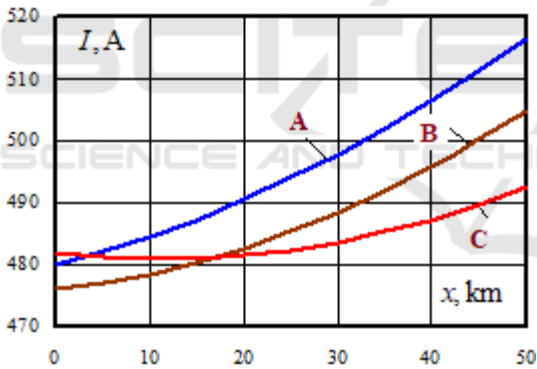


Figure 10: Currents flowing through the wires of UHV transmission line sections on the source side as a function of the x coordinate.

An important indicator characterizing the electromagnetic safety conditions is the levels of electromagnetic field strengths calculated at a height of 1.8 m, Fig. 11-13.

Since the long-distance 1,150 kV transmission line will not run through residential areas, in compliance with the current standards applicable for such a line the acceptable level of electric field (EF) strength is equal to 5 kV/m. The analysis of the obtained results allowed us to conclude that this level, in terms of the actual values, was exceeded in the range of changes in the z -coordinate that spanned

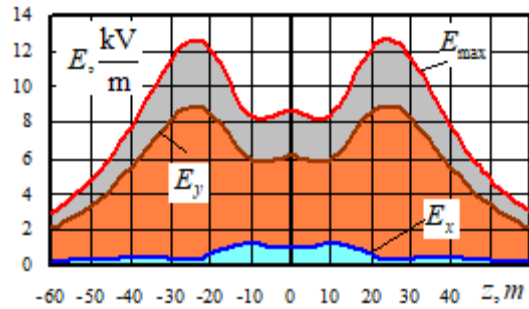


Figure 11: Electric field strength components at a height of 1.8 m as a function of the z -coordinate.

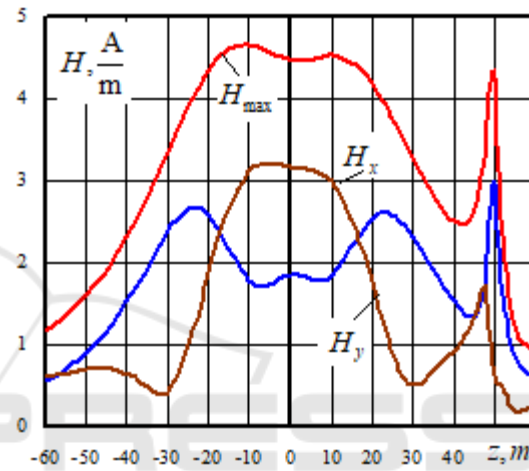


Figure 12: Magnetic field strength components at a height of 1.8 m as a function of the z -coordinate.

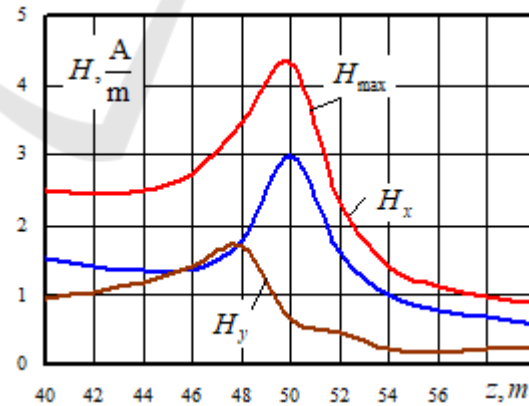


Figure 13: Magnetic field strength components at a height of 1.8 m as a function of the z -coordinate.

over $-42 \dots 42$ m. The Z axis was perpendicular to the transmission line axis. The highest values of field strength were observed directly under the line wires (Fig. 11), which was to be expected. From Fig. 12, 13 we can see that due to the current flowing through the

pipeline at the point of its location there was an increase in the magnetic field strength.

The results of determining the electromagnetic interference effects of the long-distance transmission line on the pipeline are shown in Fig. 14-17. Fig. 14 presents the dependency of induced voltages (IV) on the pipeline on the x -coordinate for the balanced load power flow. It shows that the values of induced voltages did not exceed the permissible value of 60 V established by the document (Technische Richtlinien-71). Fig. 15 shows a plot corresponding to the dependency of the current flowing through the pipe on the x -coordinate. This relationship has a maximum, which corresponds to the value of $x = 10$ km.

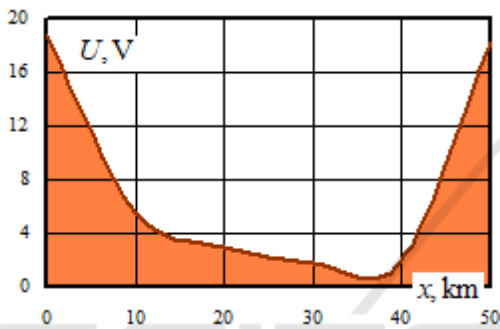


Figure 14: Induced voltages on the pipeline as a function of the x -coordinate.

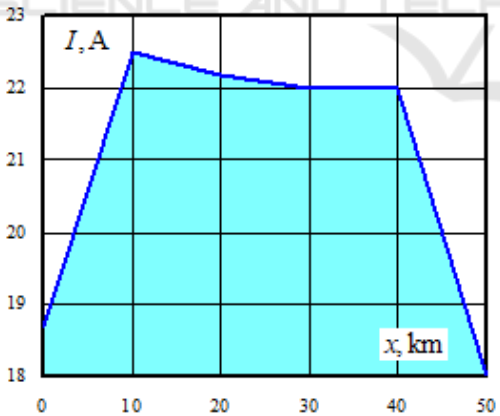


Figure 15: Currents flowing through the pipe in the case of the balanced load power flow as a function of the x -coordinate.

Fig. 16 shows the dependencies of induced voltages on the x -coordinate, obtained for unbalanced power flows, caused by switching off the shunt reactors. For certainty, we chose the reactors installed in phase A. We considered the power flows in the case of shutdowns of the reactors installed at the

points corresponding to the following values of the x -coordinate: 150, 300, 450, 600, 750 km. The asymmetry resulting from the shutting down of the reactors led to an increase in induced voltages. The greatest increase in IV was observed at the points located along the edges of the structure. The IV maximum, exceeding the permissible value of 60 V, occurred in the power flow with the shutdown of the shunt reactor installed at the point corresponding to the x -coordinate of 150 km, Fig. 17.

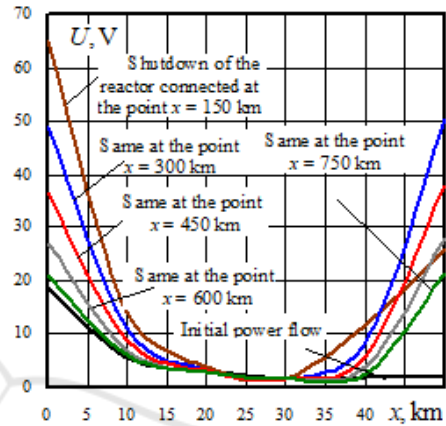


Figure 16: Induced voltages under unbalanced power flow caused by reactor shutdown in phase A as a function of the x coordinate.

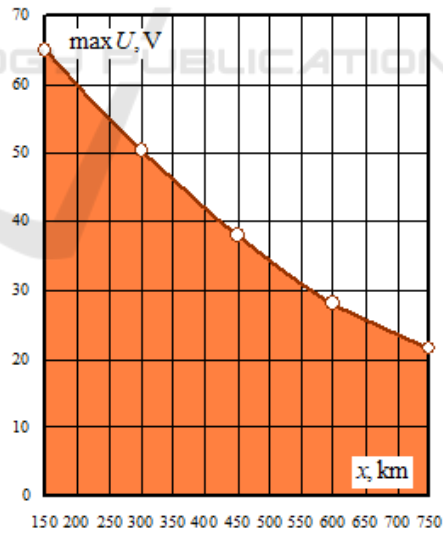


Figure 17: Maximum induced voltages in the case with reactors shut down.

Fig. 18 shows vector diagrams, built by means of the Fazonord software package, for the power flow of asymmetrical short circuits occurring at the point $x = 50$ km, which corresponds to the right end of the section where the pipeline and the transmission line

run in close proximity. From the analysis of the above diagrams, we can conclude that during a two-phase short circuit fault, the currents flowing through the phases of the transmission line had a phase shift close to 180°.

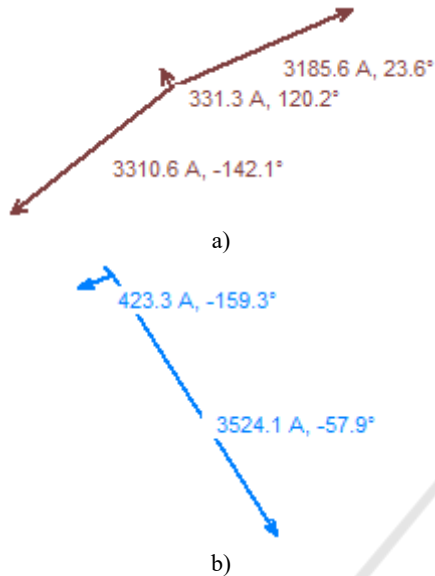


Figure 18: Vector diagrams of long-distance transmission line currents in short-circuit power flows: a - two-phase short circuit between phases C-B; b - single-phase short circuit (phase A).

Figs. 19 to 22 show the results of calculation of the induced voltages and currents flowing in the pipe during asymmetrical short circuits in the long-distance UHV transmission line. In the case of single-phase short circuits, due to a pronounced electromagnetic imbalance, the maximum induced voltages reached 700 V (Fig. 19) but did not exceed the maximum permissible value of 1,000 V, as established by the document (Technische Richtlinien-71). In this power flow, currents exceeding 800 A were flowing through the pipeline (Fig. 20). The magnitudes of the induced voltages and especially of the currents depend on the choice of the faulty phase. In the case of a single-phase short circuit, the maximum IV and currents in the pipeline were observed when phase C was shorted to ground (Fig. 20).

In the two-phase short-circuit power flow, due to the different direction of currents flowing through the current-conducting parts of the long-distance transmission line (Fig. 18), the values of induced voltages and currents in the pipe are much lower than in the case of single-phase short circuits (Fig. 21, 22).

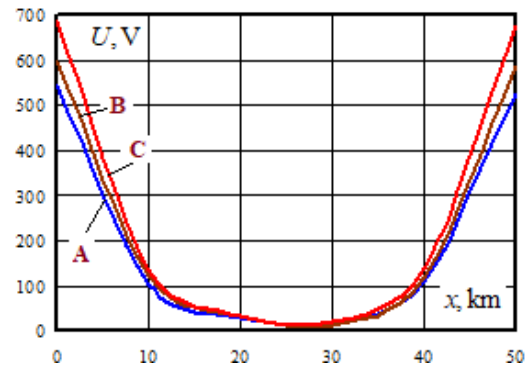


Figure 19: Induced voltages for a single-phase short circuit at the point $x = 50$ km as a function of the x -coordinate.

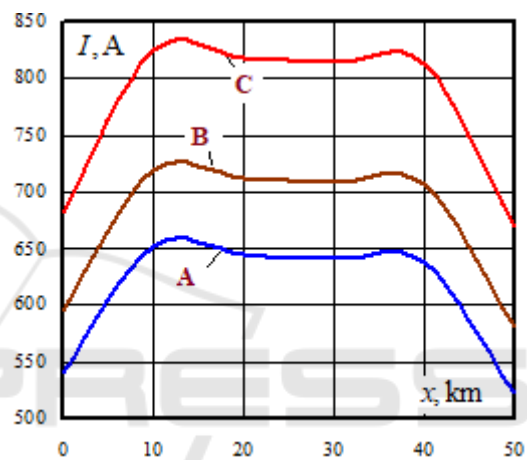


Figure 20: Currents flowing in the pipeline as a function of the x -coordinate in the case of a single-phase short circuit at the point $x = 50$ km.

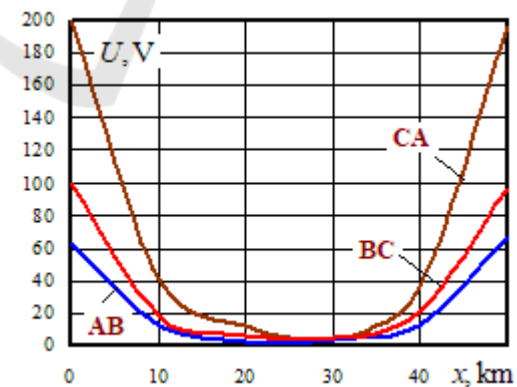


Figure 21: Induced voltages as a function of the x -coordinate in the case of a two-phase short circuit at the point $x = 50$ km.

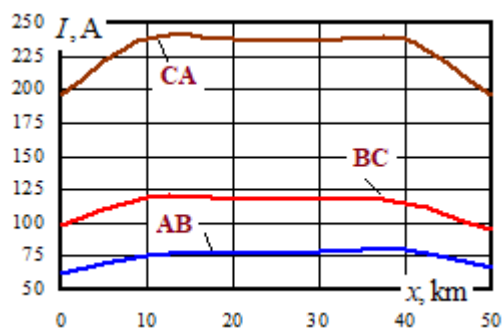


Figure 22: Currents flowing in the pipeline as a function of the x -coordinate in the case of a two-phase short circuit at the point $x = 50$ km.

4 CONCLUSIONS

We have developed digital models that allow for the comprehensive modeling of power flows of electric power systems that have long-distance ultrahigh-voltage transmission lines as their part. Furthermore, based on these models it is possible to determine EMF strengths and induced voltages occurring on the adjacent above-ground pipeline.

The results of modeling of a long-distance 1,150 kV transmission line with loads at the receiving end of $300 + j 200$ MVA per phase allowed us to draw the following conclusions:

1. Specific power losses per kilometer of transmission line ranged from 8.6 to 16.4 kW. The losses as a percentage of the transmitted active power were in the range 0.14...0.27%.
2. There was insignificant asymmetry observed at the nodal points of the long-distance transmission line, which did not exceed the permissible limits.
3. In the case of a normal power flow with balanced loads, the induced voltage levels did not exceed the permissible limit of 60 V.
4. In the case of single-phase short-circuit power flows, the maximum induced voltages reached 700 V, but did not exceed the maximum permissible value set in TRL-71. The maximum IV level occurs when phase C, whose wires were closest to the pipe, were shorted. The maximum current flowing in the pipeline reached 824 A. Because of the opposite direction of currents flowing through the current-carrying parts of the long-distance transmission line during a two-phase short-circuit, the values of induced voltages and currents in the pipe were much lower than during a single-phase short circuit. The IV maximum reached 200 V and occurred when phases CA were short-circuited. In the above case, currents of up to 240 A were flowing through the pipe.

Potential applications of the proposed models cover a rather wide range of tasks. They can provide the basis for addressing the following issues: analysis of normal, unbalanced, incomplete-phase, and non-sinusoidal power flows of electric power systems that have long-distance transmission lines as their part; analysis of electromagnetic safety conditions along the routes of such lines and substations adjoining them; choice of rational measures to protect technicians of adjacent structures located in the areas of electromagnetic interference effects of long-distance-transmission lines, etc.

The developed numerical models lend themselves to a rather straightforward modification to account also for cases where a long-distance transmission line and an adjacent steel structure run in close proximity following non-parallel trajectories.

ACKNOWLEDGEMENTS

The research was carried out within the framework of the state task "Conducting applied scientific research" on the topic "Development of methods, algorithms and software for modeling the modes of traction power supply systems for DC railways and electromagnetic fields at traction substations for AC railways".

REFERENCES

- Li, Y., He, J., Yuan, J., Chen Li, Hu, J., Zeng, R. (2013). Failure Risk of UHV AC Transmission Line Considering the Statistical Characteristics of Switching Overvoltage Waveshape. *IEEE Transactions on Power Delivery*, vol. 28, no. 3, pp. 1731 - 1739.
- Podkovalnikov S.V., Saveliev V.A., Chudinova L.Yu. (2015). Study of the systemic energy-economic efficiency of the formation of the interstate energy association of North-East Asia. *News of the Russian Academy of Sciences. Energy*. No. 5., pp. 16-32.
- Bulatov, Y., Kryukov, A., Suslov, K. (2022). Integrated Modeling of the Modes of High Voltage Long Distance Electricity Transmission Lines. In *9th International Conference on Electrical and Electronics Engineering, ICEEE 2022*, pp. 45–49.
- Wang, S., Shang, L. (2021) Research on Power Frequency Over-voltage And Suppression Measures Of Ultra-high Voltage Trans-mission Lines. In *IEEE 5th Advanced Information Technology, Electronic and Automation Control Conference (IAEAC)*, vol. 5.
- Shao, W., Wang, J., Peng, J. (2012). Reclosing Over-Voltage Analysis for Single-Phase Reclosure in UHV Transmission Lines. In *2012 Asia-Pacific Power and Energy Engineering Conference*.

- Wang, X., Xiang, Z., Li, Z. (2018). Overvoltage and Restriction of 1000kV Long-Distance Transmission Lines in Weak System. In *2nd IEEE Conference on Energy Internet and Energy System Integration (EI2)*.
- Zhang, L., Zhang, C., Shi, W., Zhang, B. (2020). Research on insulation coordination of UHV half-wavelength power transmission line. In *16th IET International Conference on AC and DC Power Transmission (ACDC 2020)*.
- Golov, V., Kalutskov, A., Kormilitsyn, D. (2020) Controlled Series Compensation of High Voltage Lines to Increase Transmission Capacity. In *International Ural Conference on Electrical Power Engineering (UralCon)*.
- Xue, S., He, J., Xu, L., Sun, J. (2011) Study of Self-Excitation Over-Voltage and Switching Over-Voltage and Their Suppression Measure in Ultra-High Long Distance Transmission Lines. In *Asia-Pacific Power and Energy Engineering Conference*.
- Xue, S., He, J., Xu, L., Wang, Y. (2011) Search scheme of self-excitation over-voltage in UHV long transmission lines. In *International Conference on Advanced Power System Automation and Protection*, vol. 2.
- Rahul, G. P., Teja, O. N., Shivani P. G., Deepa, K., Manitha, P.V., Sailaja V. (2020). Long Distance Power Transmission System with ZVS Ultra-Lift Luo Converter from Large Photovoltaic Generation. In *Third International Conference on Smart Systems and Inventive Technology (ICSSIT)*
- Long, C.S., Chun, S.H., Zhi, W.Y., Fang, Z. (2008). Distance protection scheme with traveling wave for UHVDC transmission line based on wavelet transform. In *Third International Conference on Electric Utility Deregulation and Restructuring and Power Technologies*.
- Dias, R., Lima, A., Portela, C., Aredes, M. (2011). Extra Long Distance Bulk Power Transmission. *IEEE Transactions on Power Delivery*. vol. 26. Issue 3.
- Davydov, G. I., Vasilyev, P. F. (2019). Flexible Systems for the Transmission of Electrical Energy Over Long Distances. In *International Science and Technology Conference "EastConf"*.
- Aleksandrov, G. N. (2006) Modes of operation of overhead power lines. St. Petersburg,. 138 p. (in Russian)
- Ryzhov, Yu. P. (2007). *Long-distance transmission lines of ultra-high voltage*. Moscow, 488 p. (in Russian)
- Ananicheva, S. S., Bartolomei, P. I., Myzin, A. L. *Transmission of electricity over long distances*. Ekaterinburg, 1993. 80 p. (in Russian)
- Zakaryukin, V. P., Kryukov A. V. (2005). *Complicated asymmetrical modes of electrical systems*. Irkutsk, 273 p. (in Russian)
- Zakaryukin, V. P., Kryukov, A. V., Le Thao Van (2020). *Complex modeling of multi-phase, multi-circuit and compact transmission lines*. Irkutsk,. 296 p. (in Russian)
- Kryukov, A., Suslov, K., Van Thao, L., Hung, T.D., Akhmetshin, A. (2022). Power Flow Modeling of Multi-Circuit Transmission Lines. *Energies*, vol. 15 (21), 8249.
- Technische Richtlinien-71 (TRL-71). EMR-Technic Kathodischer Korrosionsschutz für Erdgasfernleitungen. P. 80.